

## Effect of annealing temperature on the formation of Manganese doped Specialty Multiwalled carbon nanotubes (SMW-200) prepared through Solvo-thermal method

R.Ramesh kannan<sup>1,\*</sup>, S.Karthick Kumar<sup>2</sup>, M.Balaji<sup>3</sup>, S.Chandrasekaran<sup>4</sup> and M.Sivabharathy<sup>2</sup>

<sup>1</sup>Research and development Centre, Bharathiyar University, Coimbatore

<sup>2</sup>Department of Physics, Sethu Institute of Technology, Pulloor, Kariyapatti-626 115

<sup>3</sup>Department of Physics, The Sourashtra College, Madurai-625004

<sup>4</sup>School of Chemical Engineering & Bioengineering, University of Ulsan, Ulsan 680-749, Republic of South Korea.

\*Corresponding author: R.Ramesh Kannan, +919791694494

E-mail address: [rameshkannanphd@gmail.com](mailto:rameshkannanphd@gmail.com)

**Abstract:** Manganese doped Multiwalled carbon nanotubes were synthesized through a solvo thermal method. The surface morphology and structural analyses of the MnO<sub>2</sub> doped MCNT have performed by Transmission electron microscope (TEM), Field emission scanning electron microscope (FESEM), Atomic force Microscope (AFM), X-ray diffraction (XRD) and Energy dispersive spectroscopy (EDS). Fourier transform infrared (FTIR) spectrometry was used to analyze the chemical bonding and type of functional groups grafted onto the nanotubes. Morphological characterization reveals that three-dimensional hierarchy architecture built with a highly porous layer consisting of interconnected MnO<sub>2</sub> uniformly coated on the CNT surface. The XRD and EDS results confirmed that the prepared samples containing MnO<sub>2</sub>/CNT in pure form without impurities. It also reveals that birnessite-type MnO<sub>2</sub> is formed through the solvo thermal synthesis. The phase transition was take place at the annealing temperature of 400 °C – 500 °C.

**Keywords:** MWCNT, MnO<sub>2</sub>, Solvo thermal method, Nanocomposites, chemical bonding

### 1. Introduction

Carbon nanotube (CNT) is a promising candidate for electronic applications owing to outstanding electrical properties and unique charge transfer (1). Both metallic single-walled carbon nanotube (SWCNT) and multi-walled carbon nanotube (MWCNT) can transport electron ballistically over long nanotube lengths because of their one-dimensional electronic structure (2). In recent years many works have been focused on the application of CNT in super capacitors due to their electronic conductivity, high chemical stability and available specific surface area (3). CNT super capacitors have attracted considerable interest as energy storage devices of hybrid vehicles and rechargeable batteries, etc. For that we need high storage capacitance, long life cycle and low cost materials (4–6). The high storage capacitance means the larger amounts of charge injection take place when only a few volts are loaded. But pure CNT super capacitors have low specific capacitance, typically about 10–40 F/g, which mainly depend on the micro texture, purity and electrolyte (7). Therefore a number of efforts are made on improving the capacitance of CNT energy storage systems like configuration of capacitor (8–10), selection of electrolyte (11–13) and the modification of electrode (14–16). In recent years, manganese oxides (MnO<sub>2</sub>) have attracted more research interest due to their unique physical and chemical properties. It has wide applications in the field of catalysis, ion exchange, molecular adsorption, biosensor, and energy storage (17–21). Specifically, manganese dioxide has been considered as a one of the promising electrode material for super capacitors because of its low cost, environmental friendly and excellent capacitive performance in aqueous electrolytes (22–25). The charge storage in aqueous electrolytes is based either on the adsorption of cations at the surface of the electrode material or on the intercalation of cations in the bulk of the electrode material. In order to attain high capacitive performance, a large surface area and a fast ion/electron transport of the electrode material are essential (26–28). In this paper, we employed an easy in solvo thermal route to prepare morphologically uniform MnO<sub>2</sub>/MWCNT composites and further characterized their electrochemical behaviors. The effects of annealing temperature were also analyzed.

### 2. Experimental

Commercial multiwall CNTs (SMW-200) (Outer diameter: 10±1 nm, Inner diameter: 4.5±0.5 nm & Length: 3–6 μm, surface area 280–350 m<sup>2</sup>/g (BET), south west nano technologies. Inc., USA). This material produced by the Catalytic chemical vapor deposition (CCVD) method and its purity was higher than 98%. A typical synthesis process of the MnO<sub>2</sub>/CNT nanocomposite is described as follows. Firstly, 0.1 g CNTs was dispersed in 100 ml deionized water by ultrasonic vibration for 2 h. Subsequently, 0.665 g MnO<sub>2</sub> added with 15

ml of HCl and 15 ml DI water and it was mixed with above suspension. Then mixed solution was stirred by a magnetic bar for 1 hr. 15 ml of Ammonia solution was added drop by drop. Finally, the precipitation composite products were obtained through filtering, water washing and drying processes. The prepared MnO<sub>2</sub>/CNT was calcinated further at 400 and 500 °C.

### 3. Characterization

The surface morphology and structural analyses of the MnO<sub>2</sub> doped MCNT have performed by Transmission electron microscope (TEM), Field emission scanning electron microscopy (FESEM), X-ray diffraction (XRD) and Energy dispersive spectroscopy (EDS). In AFM Studies, tip bending moment force is about 4nN which is kept constant for all the samples and the morphology is obtained by silicon nitride tips with tip diameter of 10nm. The pure and oxidized CNTs samples were mixed with KBr prior to the analysis to make a pellet. FTIR spectra were recorded using Perkin Elmer instrument (Perkin Elmer) in the 4,000–400 cm<sup>-1</sup> range.

## 4. Results

### 4.1. XRD Studies

XRD patterns of the CNTs, the pure MnO<sub>2</sub> powder, and the MnO<sub>2</sub>/CNT nanocomposites are shown in Figure 1. The XRD pattern of the CNTs shows three diffraction peaks at 26.5° and 43.2° which can be indexed as the (002) and (100) reflections of graphite, respectively. The diffraction peaks which appeared at  $2\theta = 28.8^\circ$ , 37.5°, 56.2°, and 60.3° matched well with the diffraction peaks of (211), (301), (600) and (521) crystal planes of MnO<sub>2</sub> standard data (JCPDS card PDF file no. 44-0141). The lattice parameters of prepared MnO<sub>2</sub> are  $a = 9.7875$  and  $c = 2.8600$ , which are highly identical to the standard values (JCPDS card PDF file no. 44-0141,  $a = 9.7847$ ,  $c = 2.863$ ). The cell volume of caddice-clew-like MnO<sub>2</sub> is 273.97 Å<sup>3</sup> which is also highly identical to the standard values (274.1 Å<sup>3</sup>). The average grain size of the prepared MnO<sub>2</sub> crystal is calculated to be 32 nm according to the Scherrer equation  $D = K\lambda/\beta\cos\theta$  using the strongest diffraction peak of (211) where D is crystal grain size (nm), K is the Scherrer constant (0.89),  $\lambda$  is the X-ray wavelength (0.154056 nm) for Cu K $\alpha$ ,  $\beta$  is the full width at half maximum (FWHM) of the peak (211), and  $\theta$  is the angle of diffraction peak. The XRD pattern of the MnO<sub>2</sub>/CNT nanocomposite shows that the diffraction peaks from the birnessite-type MnO<sub>2</sub> phase can be observed while the diffraction peaks from the CNTs are not obvious due to the uniform coating of the MnO<sub>2</sub> layer. The XRD pattern of MnO<sub>2</sub>/CNT samples annealed at 400 and 500 °C was confirms that the while increasing the annealing temperature the crystallinity of MnO<sub>2</sub> was increased.

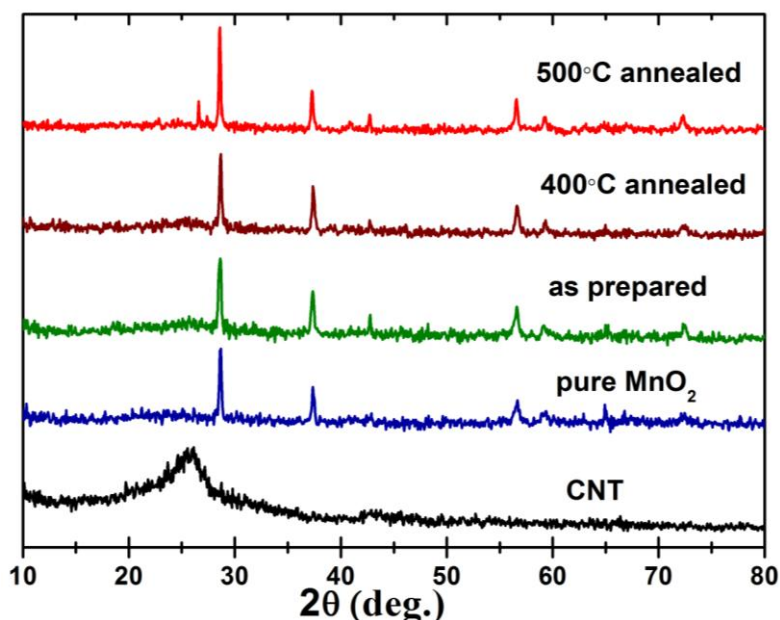


**Fig.1:** XRD patterns of the (a) pristine CNTs, (b) pure MnO<sub>2</sub>, and (c) MnO<sub>2</sub>/CNT nanocomposite.

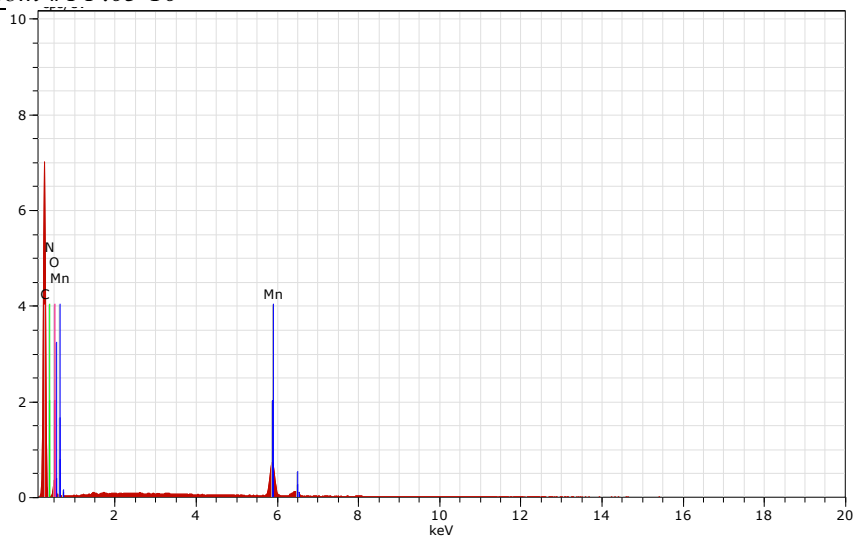


**Fig.2:** EDS spectrum of the MnO<sub>2</sub>/CNT nanocomposite.

Energy dispersive spectrum of MnO<sub>2</sub> doped MWCNT was showed in the figure 2. The results are reveals that the prepared sample has only Mn, O and C content without any impurities. When the annealing temperature was increased to 500 °C the amount of carbon content decreases while amount of MnO<sub>2</sub> content was increased. It shows that at 400 °C MnO<sub>2</sub> and CNT are in amorphous nature. it can be modified to high crystallinty. While increasing the annealing temperature to 500 °C. So we can deduce that the nanoparticles decorated on surfaces of MWNTs are MnO<sub>2</sub> doped CNT nanoparticles.

## 4.2. Morphological Studies

### 4.2.1. AFM Studies

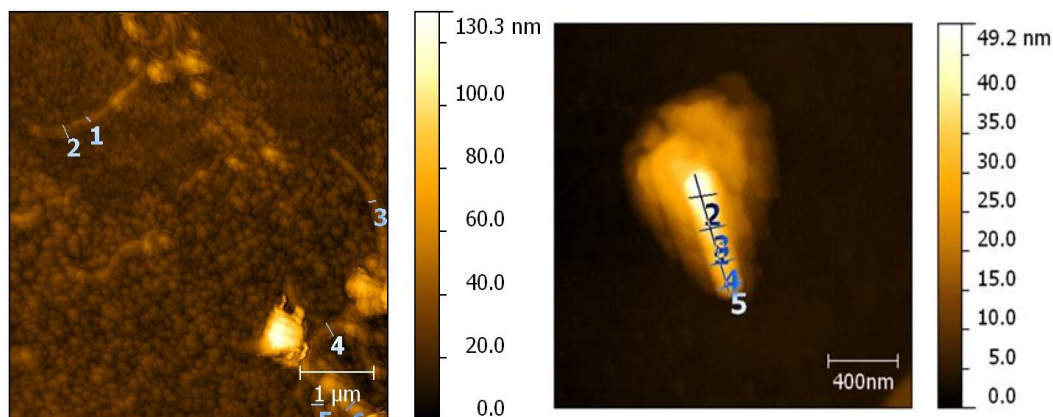


**Fig.3:** AFM images of CNT dissolved in water and methonal.

The AFM (Fig.3) images shows surface morphology of CNT dissolved in water and methanol. From the image the average diameter of CNTs was 50nm. The CNTs have very low roughness and kurtosis values while dissolving in methanol. The average roughness was decreased from 2.18 nm to 0.27 nm while changing the water to methanol. The root mean Square value was changed from 2.61 nm to 0.38 nm. It confirms that the CNT was more dissolved in methanol compare to water.

### 4.2.2. SEM and TEM Studies

Morphologies of the MnO<sub>2</sub>/CNTs nanocomposite annealed at 400 and 500 °C was characterized by FESEM (Fig. 4A&B) and TEM (Fig. 4C&D) as shown in Figure 4. It can be observed that in Figure 4A that the diameter of the CNTs is about 20 to 50 nm. When the annealing temperature was 400 °C the prepared MnO<sub>2</sub> doped MWCNT shows low number MnO<sub>2</sub> was attached with the MWCNT. While increasing the annealing temperature to 500 °C more number of MnO<sub>2</sub> particles uniformly decorated on the MWCNT (Fig.5C &D). The insert picture of TEM show that the MnO<sub>2</sub>/CNT have diameter of 26 nm.

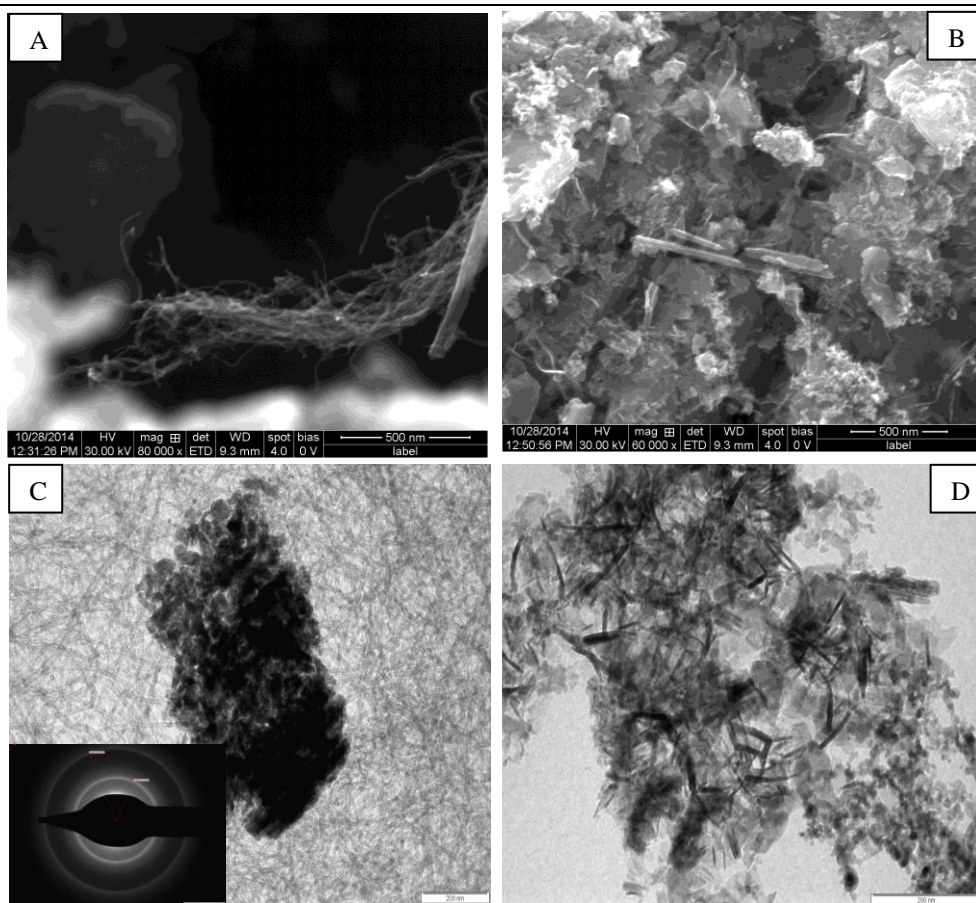


**Fig.4:** SEM images (A), (B) and (C), (D) TEM images of MnO<sub>2</sub>/CNT nanocomposite annealed at 400 °C (C) & 500 °C (D).

#### 4.3 Optical studies

The FTIR spectrum of as-prepared manganese dioxide exhibited a very broad peak centered at 3400 cm<sup>-1</sup> associated with the stretching vibration of OH groups of adsorbed water molecules. The bands at 1623 and 1415 cm<sup>-1</sup> represented the vibrations related to interactions of Mn with OH and other surface groups. The broad peak below 750 cm<sup>-1</sup> can be attributed to the vibrations of the Mn-O bonds. The peaks at 2920 and 2854 cm<sup>-1</sup> correspond to the C-H stretch vibration, originated from the surface of tubes. The intensity of peak decreases while increasing annealing temperature, which suggests that the surface of MWCNT has been covered by MnO<sub>2</sub>.



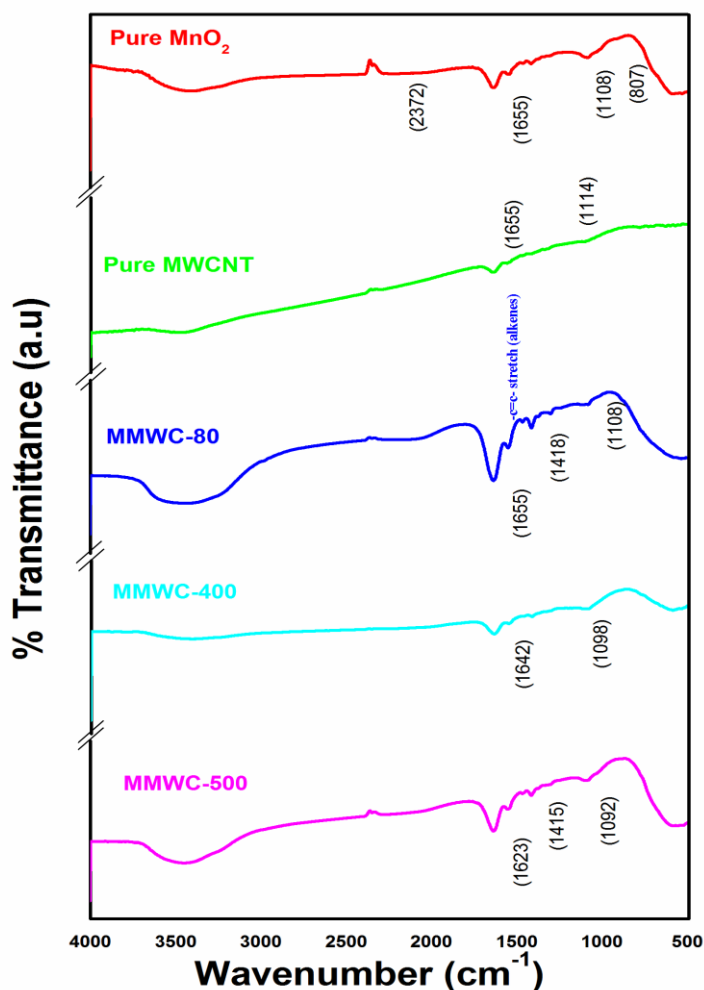


Fig.4: FTIR spectrum of prepared samples.

### 5. Conclusion

Manganese doped Multiwalled carbon nanotubes were synthesized through a solvo thermal method. The surface morphology and structural analyses of the MnO<sub>2</sub> doped MCNT were performed by Transmission electron microscope (TEM), Field emission scanning electron microscopy (FESEM), X-ray diffraction (XRD) and Energy dispersive spectroscopy (EDS). Morphological characterization reveals that three-dimensional hierarchy architecture built with a highly porous layer consisting of interconnected MnO<sub>2</sub> uniformly coated on the CNT surface. The AFM image confirms that the CNT was more dissolved in methanol compare to water. The XRD and EDS results confirmed that the prepared samples containing MnO<sub>2</sub>/CNT in pure form without impurities. It also reveals that birnessite-type MnO<sub>2</sub> is formed through the solvo thermal synthesis. The phase transition was take place at the annealing temperature of 400 °C – 500 °C. Due to their surface deposition and chemical bonding, nanocomposites are used for energy storage and electrode material in super capacitors.

### References

- [1]. Chen ZH, Appenzeller J, Lin YM, Sippel-Oakley J, Rinzler AG, Tang J. An integrated logic circuit assembled on a single carbon nanotube. *Science* 2006;311:17356.
- [2]. Baughman RH, Zakhidov AA, de Heer WA. Carbon nanotubes-the route toward applications. *Science* 2002;297:787–92.
- [3]. Beguin F, Szostak K, Lota G, Frackowiak E. A self-supporting electrode for supercapacitors prepared by one-step pyrolysis of carbon nanotube/polyacrylonitrile blends. *Adv Mater* 2005;17:2380–4.
- [4]. Khomenko V, Frackowiak E, Beguin F. Determination of the specific capacitance of conducting polymer/nanotubes composite electrodes using different cell configurations. *Electrochim Acta* 2005;50:2499–506.
- [5]. Portet C, Taberna PL, Simon P, Flahaut E. Influence of carbon nanotubes addition on carbon–carbon supercapacitor performances in organic electrolyte. *J Power Sources* 2005;139:371–8.

- [6]. Ye JS, Cui HF, Liu X, Lim TM, Zhang WD, Sheu FS. Preparation and characterization of aligned carbon nanotube-ruthenium oxide nanocomposites for supercapacitors. *Small* 2005;1:560–5.
- [7]. Lota G, Lota K, Frackowiak E. Nanotubes based composites rich in nitrogen for supercapacitor application. *Electrochem Commun* 2007;9:1828–32.
- [8]. Emmenegger Ch, Mauron Ph, Sudan P, Wenger P, Hermann V, Gallay R, Zuttel A. Investigation of electrochemical double-layer (ECDL) capacitors electrodes based on carbon nanotubes and activated carbon materials. *J Power Sources* 2003;124:321–9.
- [9]. Lee JK, Pathan HM, Jung KD, Joo OS. Electrochemical capacitance of nanocomposite films formed by loading carbon nanotubes with ruthenium oxide. *J Power Sources* 2006;159:1527–31.
- [10]. Chen QL, Xue KH, Shen W, Tao FF, Yin SY, Xu W. Fabrication and electrochemical properties of carbon nanotube array electrode for supercapacitors. *Electrochim Acta* 2004;49:4157–61.
- [11]. Portet C, Taberna PL, Simon P, Flahaut E, Laberty-Robert C. High power density electrodes for carbon supercapacitor applications. *Electrochim Acta* 2005;50:4174–81.
- [12]. Yuan AB, Zhang QL. A novel hybrid manganese dioxide/activated carbon supercapacitor using lithium hydroxide electrolyte. *Electrochem Commun* 2006;8:11738.
- [13]. Taberna PL, Chevallier G, Simon P, Plee D, Aubert T. Activated carbon-carbon nanotube composite porous film for supercapacitor applications. *Mater Res Bull* 2006;41:478–84.
- [14]. Yoon BJ, Jeong SH, Lee KH, Kim HS, Park CG, Han JH. Electrical properties of electrical double layer capacitors with integrated carbon nanotube electrodes. *Chem Phys Lett* 2004;388:170–4.
- [15]. Kim YT, Mitani T. Competitive effect of carbon nanotubes oxidation on aqueous EDLC performance: Balancing hydrophilicity and conductivity. *J Power Sources* 2006;158:1517–22.
- [16]. chemical activation. *Chem Phys Lett* 2002;361:35–41. Fei JB, Cui Y, Yan XH, Qi W, Yang Y, Wang KW, He Q, Li JB: Controlled preparation of MnO<sub>2</sub> hierarchical hollow nanostructures and their application in water treatment. *Adv Mater* 2008, 20:452.
- [17]. Liu DW, Zhang QF, Xiao P, Garcia BB, Guo Q, Champion R, Cao GZ: Hydrous manganese dioxide nanowall arrays growth and their Li<sup>+</sup> ions intercalation electrochemical properties. *Chem Mater* 2008, 20:1376-1380.
- [18]. Li ZQ, Ding Y, Xiong YJ, Yang Q, Xie Y: One-step solution-based catalytic route to fabricate novel alpha-MnO<sub>2</sub> hierarchical structures on a large scale. *Chem Commun* 2005, 7:918-920.
- [19]. Wang LZ, Sakai N, Ebina Y, Takada K, Sasaki T: Inorganic multilayer films of manganese oxide nanosheets and aluminum polyoxocations: fabrication, structure, and electrochemical behavior. *Chem Mater* 2005, 17:1352-1357.
- [20]. Hui Xia, Yu Wang, Jianyi Lin and Li Lu: Hydrothermal synthesis of MnO<sub>2</sub>/CNT Nanocomposite with a CNT core/porous MnO<sub>2</sub> sheath hierarchy architecture for supercapacitors *Nanoscale Research Letters* 2012, 7:33-43
- [21]. Chen S, Zhu JW, Han QF, Zheng ZJ, Yang Y, Wang X: Shape-controlled synthesis of one-dimensional MnO<sub>2</sub> via a facile quick-precipitation procedure and its electrochemical properties. *Cryst Growth Des* 2009, 9:4356-4361.
- [22]. Yu CC, Zhang LX, Shi JL, Zhao JJ, Cao JH, Yan DS: A simple template-free strategy to synthesize nanoporous manganese and nickel oxides with narrow pore size distribution, and their electrochemical properties. *Adv Funct Mater* 2008, 18:1544-1554.
- [23]. Hou Y, Cheng YW, Hobson T, Liu J: Design and synthesis of hierarchical MnO<sub>2</sub> nanospheres/carbon nanotubes/conducting polymer ternary composite for high performance electrochemical electrodes. *Nano Lett* 2010, 10:2727-2733.
- [24]. Xia H, Feng JK, Wang HL, Lai MO, Lu L: MnO<sub>2</sub> nanotube and nanowire arrays by electrochemical deposition for supercapacitors. *J Power Sources* 2010, 195:4410-4413.
- [25]. Liu ZP, Ma RZ, Ebina Y, Takada K, Sasaki T: Synthesis and delamination of layered manganese oxide nanobelts. *Chem Mater* 2007, 19:6504-6512.
- [26]. Umek P, Gloter A, Pregelj M, Dominko R, Jagodic M, Jaglicic Z, Zimina A, Brzhezinskaya M, Potocnik A, Filipic C, Levstik A, Arcon D: Synthesis of 3D hierarchical self-assembled microstructures formed from alpha-MnO<sub>2</sub> nanotubes and their conducting and magnetic properties. *J Phys Chem C* 2009, 113:14798-14803.
- [27]. Lili Feng, Zhewen Xuan, Hongbo Zhao, Yang Bai Junming Guo, Chang-wei Su and Xiaokai Chen MnO<sub>2</sub> prepared by hydrothermal method and electrochemical performance as anode for lithium-ion battery *Nanoscale Research Letters* 2014, 9:290
- [28]. Xiaofeng Xie, Lian Gao Characterization of a manganese dioxide/carbon nanotube composite fabricated using an in situ coating method *Science Carbon* 45 (2007) 2365– 2373